

Influence of the aggregate skeleton matrix and volumetric composition on the resistance of stone mastic asphalt to permanent deformation

Henrique Manuel Borges Miranda , Fátima Alexandra Batista , José Neves & Maria de Lurdes Antunes

To cite this article: Henrique Manuel Borges Miranda , Fátima Alexandra Batista , José Neves & Maria de Lurdes Antunes (2020): Influence of the aggregate skeleton matrix and volumetric composition on the resistance of stone mastic asphalt to permanent deformation, Road Materials and Pavement Design, DOI: [10.1080/14680629.2020.1773303](https://doi.org/10.1080/14680629.2020.1773303)

To link to this article: <https://doi.org/10.1080/14680629.2020.1773303>



Published online: 05 Jun 2020.



Submit your article to this journal [↗](#)



Article views: 11







View related articles [↗](#)



View Crossmark data [↗](#)



Influence of the aggregate skeleton matrix and volumetric composition on the resistance of stone mastic asphalt to permanent deformation

Henrique Manuel Borges Miranda ^{a,b}, Fátima Alexandra Batista ^c, José Neves ^d and Maria de Lurdes Antunes ^e

^aDepartment of Civil Engineering, ISEL – Instituto Superior de Engenharia de Lisboa, Instituto Politécnico de Lisboa, Lisbon, Portugal; ^bCITTA – Research Centre for Territory, Transports and Environment, Faculty of Engineering of the University of Porto and the Faculty of Sciences and Technology, University of Coimbra Rua Dr. Roberto Frias, Porto, Portugal; ^cPortuguese Environment Agency, Lisbon, Portugal; ^dDepartment of Civil Engineering, Architecture and Georesources, CERIS, Instituto Superior Técnico, Universidade de Lisboa, Lisbon, Portugal; ^eBoard of Directors, Laboratório Nacional de Engenharia Civil, Lisbon, Portugal

ABSTRACT

The influence of different aggregate skeleton matrices, as well volumetric composition and mixture stiffness, on the resistance of SMA to permanent deformation was assessed. Nine SMA with different optimised aggregate skeleton matrices, studied elsewhere, were now evaluated to permanent deformation with wheel tracking. The results were statistically analysed concerning relationship with specimens' volumetric characteristics, Marshall properties and mixture stiffness. Aggregate skeleton optimised with the dry rodded compaction tend to produce asphalt mixtures similar to SMA designed with pre established grading envelopes. SMA with aggregate skeleton optimised with Proctor and steel roller compaction showed higher coarse aggregates and binder contents, and thus, it is expected a better cracking resistance and durability for the same level of resistance to permanent deformation. Statistical analysis shows that the new proposed property (ratio between binder film thickness and porosity) and, ratio between Marshall stability and flow had the best correlations with permanent deformation properties.

ARTICLE HISTORY

Received 12 November 2019
Accepted 12 May 2020

KEYWORDS

Stone mastic asphalt;
stone-on-stone;
mastic-within-stone;
volumetric composition;
permanent deformation

Introduction

Stone mastic asphalt (SMA) has been, through decades, directly linked to the concept of stone-on-stone in the coarse aggregate mixture (Blazejowski, 2011; Brown & Cooley, 1999; Chelovian & Shafabakhsh, 2017; Lavin, 2003), the same way stone-on-stone effect has been linked to asphalt mixtures with higher resistance to permanent deformation (Austroads, 2009; Huber, 1999; Muraya, 2007; Pasetto & Baldo, 2014). However, what is meant with stone-on-stone effect, traditionally mentioned in the literature? Several studies address this topic, namely, through different packing models (Moghaddam & Baaj, 2018; Roquier, 2019), multi-supporting framework models (Cheng & Qin, 2019; Zhao, 2005), or multi-scale modelling (Ling & Bahia, 2020). Yet, do all SMA with a good performance, have a stone-on-stone effect? And what aggregate skeleton matrix produces the best results?

The aim of the stone-on-stone concept developed initially by Brown et al. (1998) and later standardised in AASHTO MP8 and AASHTO PP41 is to enable an asphalt mixture with a stable coarse aggregate

skeleton matrix that contributes for a higher resistance to permanent deformation. However, this approach alone does not lead a user to ensure: (i) an optimum stone-on-stone effect (optimised coarse aggregate content, since dry-rodded compaction is used) and, (ii) an optimum mastic-within-stone (volume and composition) for the correspondent air voids, which contribute to optimise SMA global performance and durability, and not just the resistance to permanent deformation.

In addition, it is widely accepted that the coarse aggregates have a major influence on the resistance to permanent deformation, yet, what are the aggregate dimensions within the coarse aggregate mixture that play the most important role? This question addressed by Zhang et al. (2019) shows that the aggregates retained on sieve sizes of 2.36 and 4.75 mm (normally used as breakpoint sieves in the stone-on-stone design) can contribute to more than 50% in the traffic load resistance. However, aggregates retained in the sieve sizes between 0.3 and 1.18 mm can provide more than 50% contribution to stabilise the stone-on-stone structure.

Furthermore, the resistance to permanent deformation depends on the individual properties of the aggregates, bitumen and additives, as well as, their interaction within the SMA.

Properties related with the aggregate shape (Jaya et al., 2014; Pan et al., 2006), or binder content and porosity (Garba, 2002; Mirzahosseini et al., 2013; Nahi et al., 2014) have been reported to have a significant influence on the resistance to permanent deformation. In another study, Jiang et al. (2017) showed that the binder properties could play a relevant role together with the gradation type or nominal maximum aggregate size. This conclusion is noteworthy due to the higher binder content usually used in the SMA, whose effect on permanent deformation will be amplified with the temperature. The interaction between the SMA constituents will be significantly ruled by the temperature, as studied by Hussan et al. (2019), comparatively to other properties such as, aggregates flakiness index, bitumen penetration and coarse aggregates content. Similar trend has also been reported by Ljubic and Prosen (2004) about the influence of bituminous mastic in the resistance to permanent deformation. This study concluded that the content of bituminous mastic is of primary importance for the resistance of SMA to permanent deformation. Too low or too high content has a great influence on that resistance, especially when compared to conventional mixtures (asphalt concrete, AC).

Therefore, new studies have been developed concerning (Miranda, 2016; Miranda et al. 2019, 2020): (1) a new laboratory aggregate compaction method to optimise the coarse aggregate skeleton, which takes into account the aggregate breakage obtained in the field; (2) a new analytical SMA mix design approach. These complementary studies have contributed to address some of the limitations of existing SMA mix design methods, based on the stone-on-stone effect, introducing a new 'mastic-within-stone' concept. The aim of the 'mastic-within-stone' concept developed by Miranda (2016) is to enable adequate bituminous mastic that contributes to improve the SMA global performance and durability. This concept together with the stone-on-stone concept, intends to work as a user guidance tool, that for an optimum aggregate skeleton matrix previously evaluated, allows to predict automatically the performance of a SMA during the mix design procedure (previously to asphalt mixture laboratory tests). This guidance tool is based on the properties and volumetric composition of each individual material used in the SMA.

To answer some of the previous concerns, the study presented in this article focused on the evaluation of the resistance of SMA to permanent deformation, concerning the influence of:

- Aggregate skeleton matrix obtained by different design methods studied in Miranda (2016) and described in Miranda et al. (2019, 2020): (i) recipe method with pre-established grading envelopes for grading selection (no skeleton matrix optimisation); (ii) optimisation procedure with manually dry-rodded method; (iii) new method using Proctor compaction (55 blows per each layer in a total of 5 equal layers) and (iv) new method using a steel roller compaction.
- Different volumetric composition (stone-on-stone and mastic-within-stone), Marshall properties and mixture stiffness for relationship establishment (statistical analysis).
- Different SMA aggregate natures and sizes.

It must be stated that this study is part of a broader research (Miranda, 2016) and deals specifically with the results obtained during the third stage, related with the evaluation of the resistance of SMA to permanent deformation.

Raw materials and test methods

Raw materials

Nine SMA with nominal maximum aggregate sizes 11, 12 and 14 mm were used. Table 1 shows the SMA identification and composition: aggregate nature; binder type and content; fibber content (bitumen coated cellulose fibber pellets).

Within a given SMA, the used materials were the same (aggregates nature, binder and fibber type), but different aggregate mix compositions were used, as well as different binder contents. The method used for mix designed was the one proposed by Miranda (2016), which is schematically represented in Figure 1.

The first phase of the developed SMA mix design method (Miranda et al., 2019) addressed the coarse aggregate skeleton matrix optimisation, using different aggregate compaction methods (Miranda et al., 2020). Thus, aggregate mix compositions were obtained with these methods (Figure 2), among which the following stand out: conventional recipe method with pre-established grading envelopes for grading selection (Gr); manual compaction with dry-rodded (Drc), consisting in applying 25 blows

Table 1. SMA identification and composition.

SMA ID	Aggregate nature	Binder type	Binder content (%)	Fibber content (%)
S11-Gr	Basalt	PMB 45/80-65	5.8	0.5
S12-Gr			5.5	0.4
S12-Drc			5.5	0.5
S12-Pro			6.5	0.5
S12-Ro	Granodiorite	PMB 45/80-55	6.5	0.5
S14-Gr/Drc ^a			6.0	0.5
S14-Pro/Ro			7.0 ^c	0.7
S14-Pro/Ro1 ^b	Basalt	PMB 45/80-65	6.5	0.6
S14-Gr1			6.0	0.4

^aSMA designed according to a grading envelope, equivalent to a SMA designed with dry-rodded manual compaction.

^bSMA designed according to Proctor compaction, equivalent to a SMA designed with steel roller compaction.

^c0.5% above optimum binder content.

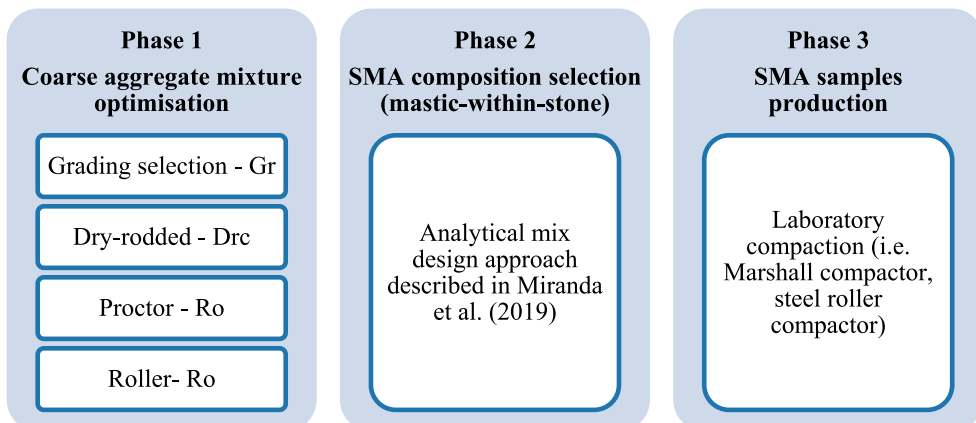


Figure 1. SMA design method used in the study.

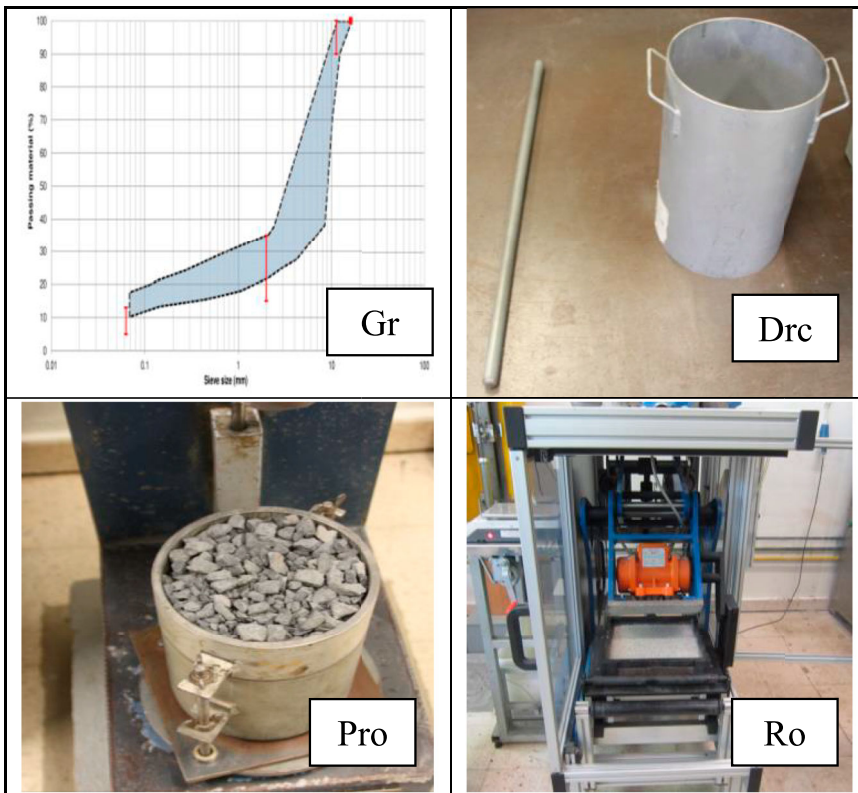


Figure 2. Aggregate compaction methods.

per layer in a total of 3 layers; Proctor compaction (Pro), applying 55 blows (4.54 kg) per layer in a total of 5 layers; and steel roller compaction (Ro) using 15 rolling cycles with vibration.

Phase 2 of the new design method (Miranda et al., 2019) aims at the volumetric selection of the remaining SMA materials (mastic-within-stone) and porosity. This volumetric composition is based on the coarse aggregate volume evaluated in phase 1 (whose content in the asphalt mixture depends on the compaction method used). The aggregate skeleton matrix (type stone-on-stone) is obtained when the air void volume in the coarse aggregate of a compacted SMA (VCA_{MIX}) is approximately the same as the air void volume in the compacted skeleton of coarse aggregates (VCA) compacted in the laboratory by one of the methods used in phase 1.

Table 2 presents the VCA from coarse aggregate specimens (material retained in breakpoint sieve equal to 4 mm) prepared by the different compaction methods.

Moreover, Figures 3 and 4 show, respectively, the SMA grading curves and aggregate skeleton matrix obtained for each SMA evaluated in this study concerning the resistance to permanent deformation.

All SMA produced in this study, except the S12-Gr, visually (Figure 4) show a good stone-on-stone effect, independently of coarse aggregate skeleton matrix optimisation previously made in Miranda et al. (2019).

Performance test programme

Resistance to permanent deformation was evaluated with wheel tracking tests on conventional and optimised stone-on-stone SMA mixes. The tests were performed according to the procedure B in air, as per in EN 12697-22 (SSD – Small Size Device), on prismatic specimens with 300 mm × 300 mm ×

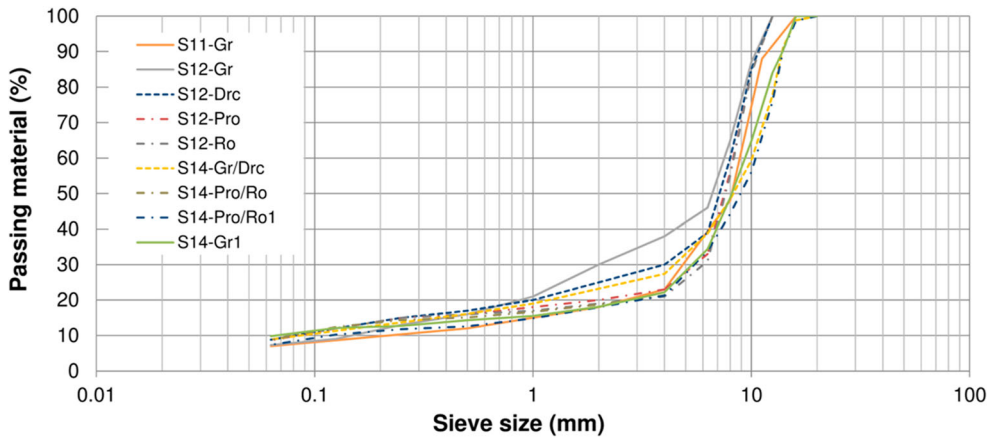
Table 2. Air voids content in the coarse aggregate.

Aggregate compaction method	Aggregate nature	Air voids content (VCA, %)
Dry-rodged (Drc) ^a	Granodiorite	43.0
	Basalt	42.0
	Granite	43.1
Proctor (Pro) ^b	Granodiorite	37.5
	Basalt	38.9
	Granite	36.3
Steel roller (Ro) ^c	Granodiorite	36.1
	Basalt	40.5
	Granite	41.7

^a25 blows per layer in a total of 3 layers, manual procedure.

^b55 blows (4.54 kg) per layer in a total of 5 layers.

^c15 rolling cycles with vibration.

**Figure 3.** SMA grading curves.**Figure 4.** SMA aggregate skeleton matrix.

50 mm produced by laboratory steel roller compactor and conditioned at 60°C. Maximum rut depth (RD_{AIR}), maximum wheel tracking slope (WTS_{AIR}) and maximum proportional rut depth (PRD_{AIR}), were evaluated after 10,000 load cycles.

In addition, Marshall and stiffness tests carried out by Miranda (2016) on the same SMA mixes used in this study were considered. The mixes Marshall stability, flow and Quotient were evaluated according to EN 12697-34 test method. The stiffness of these mixes was determined using four-point bending test on prismatic specimens (4PB-PR), according to the method described in the Annex B of EN 12697-26.

Volumetric composition

A statistical analysis was carried out in order to evaluate the relationship between the resistance of SMA to permanent deformation (RD_{AIR} , WTS_{AIR} , PRD_{AIR}) and specimen's volumetric characteristics according to Pearson's product-moment correlation.

The analysis considers also binder film thickness (BFT), calculated according to the method described in Shell (2015) and a new property, herein, represented by the ratio between binder film thickness (BFT) and porosity (V_v) in the compacted SMA.

In theory, for each SMA it is expected that an optimum binder film thickness will lead to an optimised resistance to permanent deformation. However, this resistance is also dependent, namely, of the porosity obtained in the compacted SMA. Therefore, it is proposed that the resistance to permanent deformation can be optimised through the ratio between BFT and V_v (Figure 5).

According to Figure 5, a specific ratio between binder film thickness and porosity should be used in order to optimise resistance to permanent deformation, represented by the red dot.

Packing characteristics of the designed SMA were also analysed by means of the three ratios specified in Bailey method (Vavrik et al., 2001; Vavrik et al., 2002; Voskuilen, 2000): the coarse aggregate particles ratio (CA_{ratio}); the fine aggregate coarse particles ratio (FA_{cratio}); and the fine aggregate fine particles ratio (FA_{fratio}). The three ratios can be calculated using the following equations:

$$CA_{ratio} = \frac{\% \text{ passing half sieve} - \% \text{ passing PCS}}{100\% - \% \text{ passing half sieve}} \quad (1)$$

PCS is the primary control sieve defined as the closest sieve to the numerical result obtained with the equation:

$$PCS = 0.22 \text{ NMPS} \quad (2)$$

NMPS is the nominal maximum particle size (sieve larger than the first sieve that retains more than 10%).

$$FA_{cratio} = \frac{\% \text{ passing SCS}}{\% \text{ passing PCS}} \quad (3)$$

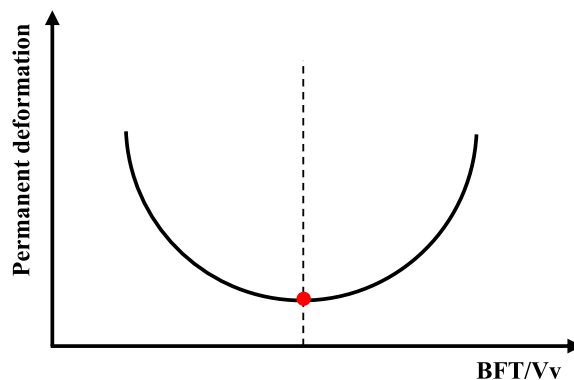


Figure 5. Proposed optimisation of resistance to permanent deformation as a function of BFT/ V_v .

Table 3. Statistical analysis of SMA properties.

SMA Property		Property ID	Transformation
Volumetric	Nominal maximum aggregate size	D	-
	Coarse aggregate content	CA	Square root
	Fine aggregate content	FA	Square root
	Filler content	F	-
	Binder content	B	-
	Ratio between filler and binder	F/B	-
	Binder film thickness	BFT	-
	Ratio between binder film thickness and porosity	BFT/Vv	-
	Porosity	Vv	-
	Volume of binder	Vb	-
	Air voids in the aggregate structure	VMA	-
	Air voids filled with binder	VFB	-
	Packing characteristics (Bailey method)	Percentage passing in the primary control sieve	PCS
Coarser aggregate particles ratio		CA _{ratio}	-
Fine aggregate coarse particles ratio		FA _{cratio}	-
Marshall	Fine aggregate fine particles ratio	FA _{fratio}	-
	Stability	S	-
	Flow	f	-
Performance	Ratio between stability and flow	Q	Square root
	Stiffness ^a	E	Square root
	Maximum rut depth, in air	RD _{AIR}	Inverse
	Maximum wheel tracking slope, in air	WTS _{AIR}	-
	Maximum proportional rut depth, in air	PRD _{AIR}	Inverse

^aTests were performed, in Miranda (2016), according to the four-point bending test procedure described in the EN 12697-26, except for mixtures S12-Drc, S14-Pro/Ro and S14-Gr1 due to material restriction. The stiffness tests were performed under controlled strain, using a 10 Hz sinusoidal load, at 20°C.

SCS is the secondary control sieve, obtained by multiplying the PCS by the 0.22 factor.

$$FA_{\text{ratio}} = \frac{\% \text{ passing TCS}}{\% \text{ passing SCS}} \quad (4)$$

TCS is the tertiary control sieve (TCS), obtained by multiplying the SCS by the 0.22 factor. The statistical analysis was, moreover, complemented with Marshall properties and mixture stiffness derived from Miranda (2016) for the same SMA mixes used in this study.

Table 3 shows the SMA properties and their denominations used in the analysis.

Properties in Table 3 were tested for linear relationship between variables, significant outliers and normality (transformations were applied when required). Furthermore, a correlation rank was established between listed SMA properties and: (i) maximum rut depth (RD_{AIR}), (ii) maximum wheel tracking slope (WTS_{AIR}) and, (iii) maximum proportional rut depth (PRD_{AIR}), evaluated according to the test method previously described.

Results

This section presents the experimental testing results considering SMA with different coarse aggregate skeletons, resulting from the optimisation developed in Miranda et al. (2019). Table 4 shows the SMA volumetric properties and aggregate packing characteristics results derived from different coarse aggregate optimisation methods used in Miranda et al. (2019). In addition, Table 5 shows the Marshall results and Table 6 and Figure 6 show the permanent deformation and mixture stiffness results.

A Pearson's product-moment correlation was run to assess the relationship between the multiple SMA properties (Table 3) and: (i) RD_{AIR}, (ii) WTS_{AIR} and (iii) PRD_{AIR}.

Preliminary analysis showed the relationship to be linear with variables normally distributed, as assessed by Shapiro-Wilk's test ($p > 0.05$), and there were no outliers. Table 7 and Figures 7 and 8

Table 4. SMA volumetric properties and coarse aggregate packing characteristics.

SMA ID	Binder content ^a (%)	CA content ^c (%)	FA content ^d (%)	Filler content ^e (%)	F/B BFT (μm)		VCA _{MIX} /VCA	Bailey method		
								CA ratio ^f	FAC ratio ^g	FAf ratio ^h
S11-Gr	5.8	72.1	15.0	6.6	1.1	11.5	0.92	0.11	0.66	0.63
S12-Gr	5.5	58.3	28.9	6.9	1.2	9.1	1.11	0.29	0.54	0.58
S12-Drc	5.5	65.9	19.8	8.3	1.5	7.9	0.95	0.24	0.68	0.72
S12-Pro	6.5	71.4	13.6	8.0	1.2	9.7	0.99	0.21	0.80	0.77
S12-Ro	6.5	73.2	11.6	8.2	1.3	9.7	0.99	0.19	0.84	0.78
S14-Gr/Drc	6.0	68.2	17.0	8.3	1.4	9.0	1.00	0.26	0.70	0.70
S14-Pro/Ro	7.0 ^b	72.8	11.4	8.1	1.2	10.7	0.98	0.23	0.79	0.81
S14-Pro/Ro1	6.5	73.1	12.9	6.9	1.1	11.3	0.97	0.24	0.72	0.78
S14-Gr1	6.0	72.8	11.6	9.2	1.5	8.9	0.83	0.25	0.77	0.85

Abbreviations: CA: coarse aggregate; FA: fine aggregate; F/B: ratio between filler and binder; BFT: binder film thickness; VCA_{MIX}/VCA: ratio between the air void volume in the coarser aggregate of a compacted SMA and the air void volume in the compacted skeleton of coarser particles; CA ratio: coarser aggregate particles ratio; FAC ratio: fine aggregate coarse particles ratio; FAf ratio: fine aggregate fine particles ratio.

^aoptimum binder content.

^b0.5% above optimum binder content.

^cparticles with dimension equal or higher than the breakpoint sieve 4 mm.

^dparticles with dimension between breakpoint sieve 4 mm and sieve 0.063 mm.

^eparticles with dimension below sieve 0.063 mm.

^frecommended range: 0.25–0.40.

^grecommended range: 0.60–0.85.

^hrecommended range: 0.60–0.85.

Table 5. Marshall results.

SMA ID	Specimen's volumetric properties					Marshall properties		
	Vv (%)	Vb (%)	VMA (%)	VFB (%)	BFT/Vv	Stability, S (kN)	Flow, f (mm)	Ratio Stability/Flow, Q (kN/mm)
S11-Gr	3.4	14.2	17.7	80.5	3.7	12.3	3.8	3.3
S12-Gr	3.1	13.1	16.2	80.6	3.2	15.9	5.1	3.1
S12-Drc	2.0	13.0	15.0	86.7	4.3	14.5	4.9	3.0
S12-Pro	3.4	15.1	18.6	81.6	3.0	11.7	3.9	3.0
S12-Ro	3.5	15.1	18.7	80.8	2.9	9.6	3.6	2.7
S14-Gr/Drc	2.8	14.8	17.7	83.6	3.3	9.4	6.5	1.5
S14-Pro/Ro	2.2	17.2	19.4	88.7	5.6	10.8	5.1	2.2
S14-Pro/Ro1	3.1	16.0	19.1	84.0	3.7	9.5	3.1	3.0
S14-Gr1	2.9	13.7	16.6	82.7	3.5	8.2	2.4	3.5

Abbreviations: Vv: porosity of the compacted SMA; Vb: volume of binder; VMA: air voids in the aggregate structure; VFB: air voids filled with binder; BFT/Vv: ratio between binder film thickness and porosity.

present the results of the Pearson correlation coefficients (r) for SMA properties, and rank the five best correlations.

Discussion

The results of the resistance to permanent deformation are discussed below regarding: (i) the influence of the aggregate skeleton matrix obtained by different coarse aggregate optimisation methods, derived from Miranda et al. (2019); and (ii) the statistical relationship with the SMA volumetric properties, Marshall and stiffness properties.

Influence of the aggregate skeleton matrix

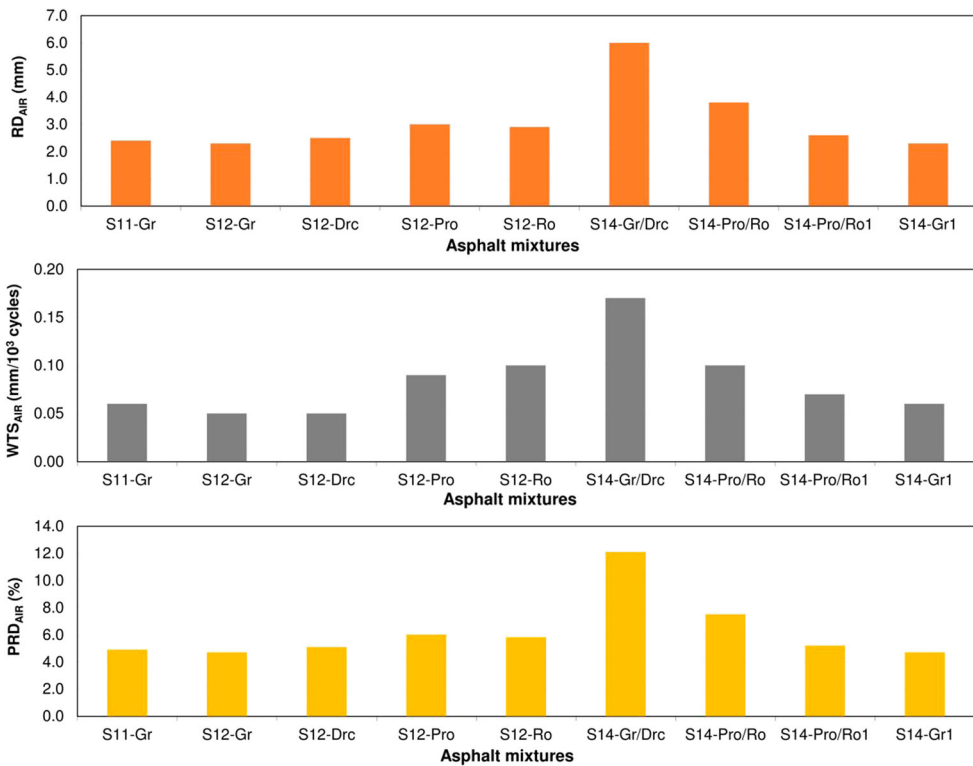
In Miranda et al. (2019), Proctor (55 blows per each layer, 5 equal layers) showed the best results when used to: (i) evaluate specimens' bulk densities, (ii) stone-on-stone particles contact and SMA volumetric

Table 6. Permanent deformation and stiffness results.

SMA ID	Specimen's volumetric properties					Permanent deformation properties (60°C)			Stiffness (10 Hz, 20°C)
	Vv (%)	Vb (%)	VMA (%)	VFB (%)	BFT/Vv	RD _{AIR} (mm)	WTS _{AIR} (mm/10 ³ cycles)	PRD _{AIR} (%)	E ^a (MPa)
S11-Gr	5.2	14.0	19.2	73.0	2.4	2.4	0.06	4.9	3908
S12-Gr	3.9	13.0	16.9	76.8	2.5	2.3	0.05	4.7	3156
S12-Drc	2.2	13.0	15.1	85.8	3.9	2.5	0.05	5.1	-
S12-Pro	2.6	15.3	17.9	85.5	4.0	3.0	0.09	6.0	3161
S12-Ro	2.9	15.2	18.1	84.2	3.6	2.9	0.10	5.8	3248
S14-Gr/Drc	1.5	15.0	16.5	90.9	6.3	6.0	0.17	12.1	3827
S14-Pro/Ro	2.5	17.2	19.6	87.5	5.0	3.8	0.10	7.5	-
S14-Pro/Ro1	3.2	16.0	19.2	83.5	3.6	2.6	0.07	5.2	3839
S14-Gr1	3.5	13.7	17.2	79.6	2.9	2.3	0.06	4.7	-

Abbreviations: RD_{AIR}: maximum rut depth, in air; WTS_{AIR}: maximum wheel tracking slope, in air; PRD_{AIR}: maximum proportional rut depth, in air; E: asphalt mixture stiffness.

^aResults for statistical analysis propose only in this study, derived from the broader research study developed in Miranda, 2016, which will be further studied in a specific article.

**Figure 6.** Wheel tracking results for 10,000 load cycles at 60°C.

properties, as well as (iii), better representation of field results in terms of particle breakage [as studied by Miranda (2016) and described in Miranda et al. (2020)]. SMA with coarse aggregate optimised with Proctor and steel roller compaction resulted in asphalt mixtures with higher coarse aggregates content and binder content (around 1.0%), comparatively to SMA designed by recipe method or optimised with the dry-rodded compaction (Table 4). This led to asphalt mixtures with lower Marshall stability (S) and flow (f), as shown in Table 5, possibly due to, respectively, the higher binder content used and

Table 7. Statistical analysis for SMA properties.

SMA property	RD _{AIR}		WTS _{AIR}		PRD _{AIR}		
	<i>r</i>	Rank	<i>R</i>	Rank	<i>r</i>	Rank	
D	-0.455	-	-0.428	-	-0.449	-	
B	-0.451	-	0.382	-	-0.417	-	
CA	-0.186	-	0.215	-	-0.163	-	
FA	0.251	-	-0.273	-	0.229	-	
F	-0.299	-	0.316	-	-0.304	-	
F/B	0.030	-	0.017	-	0.004	-	
BFT	0.008	-	-0.023	-	0.031	-	
BFT/Vv	-0.939 ^b	2	0.878 ^b	2	-0.939 ^b	2	
Vv	0.723 ^a	4	-0.642	-	0.719 ^a	4	
Vb	-0.601	-	0.510	-	-0.570	-	
VMA	-0.048	-	0.019	-	-0.020	-	
VFB	-0.805 ^b	3	0.716 ^a	3	-0.796 ^a	3	
Bailey method	PCS	0.113	-	-0.150	-	0.092	-
	CA ratio	-0.140	-	0.106	-	-0.147	-
	FAc ratio	-0.330	-	0.344	-	-0.305	-
	FAf ratio	-0.169	-	0.152	-	-0.147	-
Marshall method	S	0.375	-	-0.496	-	0.364	-
	f	-0.673 ^a	5	0.566	-	-0.690 ^b	5
	Q	0.963 ^b	1	-0.912 ^b	1	0.966 ^b	1
E	-0.243	-	0.233	-	-0.251	-	

Abbreviations: D: nominal maximum aggregate size; CA: coarse aggregate content; FA: fine aggregate content; F: filler content; B: binder content; F/B: ratio between filler and binder; BFT: binder film thickness; BFT/Vv: ratio between binder film thickness and porosity; Vv: porosity of the compacted SMA; Vb: volume of binder; VMA: air voids in the aggregate structure; VFB: air voids filled with binder; PCS: percentage passing in the primary control sieve; CA ratio: coarser aggregate particles ratio; FAc ratio: fine aggregate coarse particles ratio; FAf ratio: fine aggregate fine particles ratio; S: stability; f: flow; Q: ratio between Marshall stability and flow; E: asphalt mixture stiffness.

^astatistically significant at $p < 0.05$ level.

^bstatistically significant at $p < 0.005$ level.

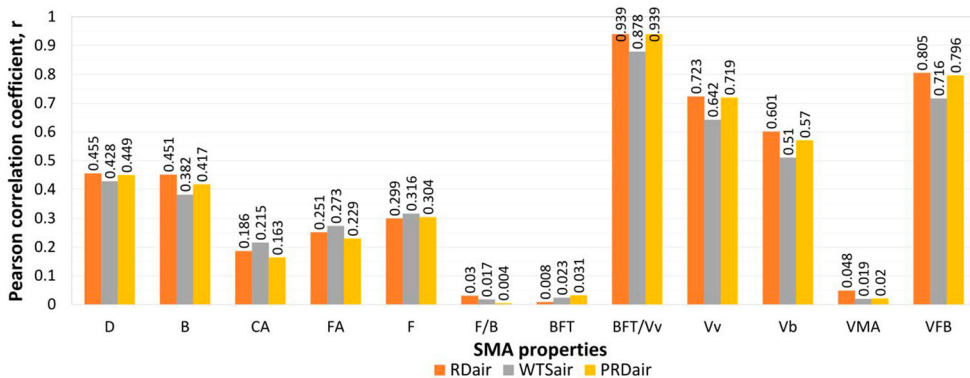


Figure 7. Pearson correlation coefficients for SMA volumetric properties with RD_{AIR}, WTS_{AIR} and PRD_{AIR}.

improved stone-on-stone aggregate skeleton matrix. However, the ratio between Marshall stability and flow (Q), did not show evident differences among the SMA with distinct coarse aggregate skeleton matrices. Similar results were attained for the asphalt mixture stiffness (E), as shown in Table 6, without any evident differences between SMA with distinct aggregate skeleton matrices. The results of Q and

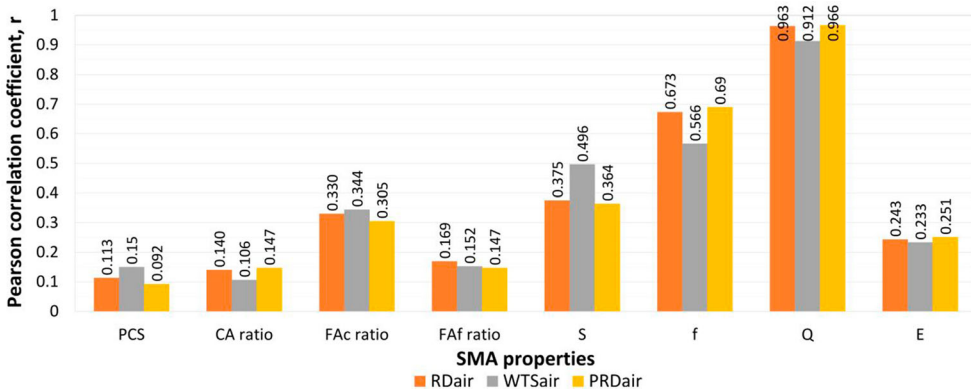


Figure 8. Pearson correlation coefficients for SMA properties (packing characteristics, Marshall & performance) with RD_{AIR} , WTS_{AIR} and PRD_{AIR} .

E, may be related, as previously mentioned, to the higher binder content used, which mitigate the effect of the higher coarse aggregate content, and therefore increase the SMA flexibility.

Nevertheless, despite the differences between properties of the asphalt mixtures studied, the results in Table 6 show that a good resistance to permanent deformation characterised all SMA. The exception was S14-Gr/Drc with a RD_{AIR} equal to 6.0 mm, probably due to lower porosity, 1.5%.

The best permanent deformation performance was assessed for SMA's designed according to recipe method or optimised with dry-rodded compaction. These results highlight the importance of fine aggregates within the coarse aggregate structure as shown by Zhang et al. (2019). However, this SMA's, as shown in Table 4, tend to have lower coarse aggregate content (CA), as well as, lower binder content ($< 6.0\%$) and VMA ($< 17.0\%$), comparatively to SMA optimised with Proctor and steel roller compaction. Thus, resulting in asphalt mixtures with thinner binder film coatings. These results may lead furthermore, to SMA with reduced performance for other areas such as fatigue ageing resistance and water sensitivity, and ultimately durability.

Moreover, the resistance to permanent deformation tends to be not significantly affected in SMAs optimised with Proctor and steel roller compaction, despite the higher binder content used, comparatively to SMAs designed by recipe method or optimised with dry-rodded compaction. That is particularly evident for S14-Pro/Ro which has a binder content 0.5% above the optimum content, as a result of an improved stone-on-stone aggregate skeleton matrix.

In addition, the resistance to permanent deformation does not appear to be affected by non-compliance with the ranges for aggregate ratios (CA_{ratio} , FA_{cratio} and FA_{fratio}) recommend in the Bailey method (Table 4). Results show that for all asphalt mixtures, except S14-Gr/Drc and S14-Gr1, at least one of the recommend ranges was not satisfied. Despite that fact, all SMA in Table 6 showed a good resistance to permanent deformation.

These results demonstrate the importance of: (i) the type of aggregate skeleton matrix (obtained according to the design method used), (ii) the binder content, and (iii) the porosity, in the resistance of SMA to permanent deformation.

Statistical relationship with the SMA volumetric properties, Marshall and stiffness properties

The results in Table 7 and Figures 7 and 8 show that the coarse aggregate content (CA) and nominal maximum aggregate size (D) do not show a statistically significant correlation with permanent deformation properties. Therefore, the use of a higher coarse aggregate content, which contributes to increase the effect of the stone-on-stone, statistically may not necessarily result on SMA with higher resistance to permanent deformation, depending on other characteristics of the mix. Additionally,

according to Table 7, there was a statistically significant, medium to strong correlation between: (i) Q, (ii) BFT/Vv, (iii) VFB, (iv) Vv, (v) f and RD_{AIR} and PRD_{AIR} , with Q explaining 93% of the variation in RD_{AIR} and PRD_{AIR} and the least (f) only 45% and 48%, respectively.

When considering WTS_{AIR} only three properties stand out from the remaining, with a statistically significant, strong correlation between: (i) Q, (ii) BFT/Vv, (iii) VFB and WTS_{AIR} , with Q explaining 83% of the variation in WTS_{AIR} and the least (VFB) only 51%.

From all the properties analysed in this study, the new property proposed in this study (ratio between binder film thickness and porosity, BFT/Vv) showed a statistically significant strong correlation with RD_{AIR} and PRD_{AIR} and WTS_{AIR} , explaining 77% of the variation in WTS_{AIR} and 88% in RD_{AIR} and PRD_{AIR} .

Since there is a very strong correlation between Q (ratio between Marshall stability and flow) and the permanent deformation properties (91% of the variation in WTS_{AIR} and 96% and 97% in RD_{AIR} and PRD_{AIR} , respectively), this means that this parameter can be used for a preliminary verification of the SMA performance with respect to permanent deformation.

Conclusions

In this paper the resistance to permanent deformation of SMA was assessed regarding: (i) the influence of the aggregate skeleton matrix obtained by different coarse aggregate optimisation methods, derived from Miranda et al. (2019); and (ii) the statistical relationship with the SMA volumetric properties, Marshall and stiffness properties.

The results allow to achieve the following main conclusions:

- SMA with coarse aggregate optimised with Proctor did not clearly distinguish itself from the dry-rodded and steel roller compaction, with respect to the SMA's resistance to permanent deformation.
- For the studied cases, SMA tended to show a good resistance to permanent deformation with similar results independently: (i) of the aggregate skeleton matrix design method used, or (ii) of non-compliance with aggregate ranges recommended in the Bailey method.
- SMA optimised with Proctor and steel roller compaction tended to ensure a higher coarse aggregate content, higher binder content (around 1.0%), and VMA, as well as a thicker binder film coating comparatively to SMA designed by recipe method or optimised with dry-rodded compaction. Nevertheless, their resistance to permanent deformation was not significantly affected, despite the higher binder content.
- The use of a higher coarse aggregate content or nominal maximum aggregate size did not show a statistically significant correlation with the resistance to permanent deformation.
- Ratio between Marshall stability and flow, as well as, the ratio between binder film thickness and porosity revealed to have a statistically significant strong correlation with permanent deformation properties (RD_{AIR} , WTS_{AIR} and PRD_{AIR}).

The research described in this paper corresponds to the third stage of a broader study reported in Miranda (2016). It regards the evaluation of the resistance to permanent deformation for different SMA designed according to the new analytical mix design approach described in Miranda et al. (2019), using new aggregate compaction methods described in Miranda et al. (2020) for coarse aggregate skeleton optimisation.

Finally, the results achieved in this research will contribute to the optimisation of SMA mix design in order to achieve improved performance in terms of fatigue, ageing resistance, water sensitivity and durability, without compromising resistance to permanent deformation. The results showed that stone-on-stone concept should be complemented with a new concept, named in Miranda (2016) as 'mastic-within-stone' This new concept intends to contribute for a suitable selection of the bituminous mastic (volume and composition) in order to optimise not only the resistance to permanent

deformation, but SMA global performance (mechanical and functional) and ultimately durability. Further studies are recommended in order to validate the concept for SMA with other constituents.

Acknowledgements

The authors wish to acknowledge the Rettenmaier Ibérica S.L. Y CIA. S. COM. company for providing some of the materials used in the research described in this article.

Disclosure statement

No potential conflict of interest was reported by the author(s).

ORCID

Henrique Manuel Borges Miranda  <http://orcid.org/0000-0003-4062-1402>

Fátima Alexandra Batista  <http://orcid.org/0000-0001-7563-8744>

José Neves  <http://orcid.org/0000-0002-7131-7967>

Maria de Lurdes Antunes  <http://orcid.org/0000-0002-1911-517X>

References

- AASHTO MP8. Standard specification for designing stone matrix asphalt (SMA). American Association of State and Highway Transportation Officials.
- AASHTO PP41. Standard practice for designing stone matrix asphalt (SMA). American Association of State and Highway Transportation Officials.
- Austroroads. (2009). *Review of stone mastic asphalt design concepts (Report No. AP-T138/09)*. Austroroads Incorporated.
- Blazejowski, K. (2011). *Stone matrix asphalt: Theory and practice*. CRP Press, Taylor & Francis Group.
- Brown, E. R., & Cooley, L. A. (1999). *Designing stone matrix asphalt mixtures for rut-resistant pavements (Report No. NCHRP 425)*. National Center for Asphalt Technology (NCAT) and National Cooperative Highway Research Program.
- Brown, E. R., Haddock, J. E., Crawford, C., Hughes, C. S., Lynn, T. A., Cooley, L. A., & Mallick, R. B. (1998). *Designing stone matrix asphalt mixtures: Volume I – literature review; volume II (A) – research results for part 1 of phase I; volume II(B) – research results for part 2 of phase I; volume II(C) – research results for phase II; volume III – summary of research results; volume IV – mixture design method, construction guidelines, and quality control procedures; and volume V – appendix for phase II work. (Report No. NCHRP 9-8 Final Report)*. National Center for Asphalt Technology (NCAT) and National Cooperative Highway Research Program.
- Chelovian, A., & Shafabakhsh, G. (2017). Laboratory evaluation of Nano Al₂O₃ effect on dynamic performance of stone mastic asphalt. *International Journal of Pavement Research and Technology*, 10, 131–138. <https://doi.org/10.1016/j.ijprt.2016.11.004>
- Cheng, Y., & Qin, Y. (2019). Aggregates breakage introduction to optimize gradation of multi-supporting skeleton asphalt mixtures. *Construction and Building Materials*, 200, 265–271. <https://doi.org/10.1016/j.conbuildmat.2018.12.118>
- EN 12697-22. *Bituminous mixtures – test methods for hot mix asphalt – part 22: Wheel tracking*. European Committee for Standardization.
- Garba, R. (2002). *Permanent deformation properties of asphalt concrete mixtures* (Doctoral dissertation). Norwegian University of Science and Technology, Norway. <hdl.handle.net/11250/231328>
- Huber, G. A. (1999). *Methods to achieve rut-resistant durable pavements. (Synthesis of Highway Practice 274)*. Transportation Research Record and National Cooperative Highway Research Program.
- Hussan, S., Kamal, M. A., Hafeez, I., Farooq, D., Ahmad, N., & Khanzada, S. (2019). Statistical evaluation of factors affecting the laboratory rutting susceptibility of asphalt mixtures. *International Journal of Pavement Engineering*, 20(4), 402–416. <https://doi.org/10.1080/10298436.2017.1299527>
- Jaya, R. P., Hassan, N. A., Mahmud, M. Z. H., Aziz, M. A., Hamzah, M. O., & Wan, C. N. C. (2014). Effect of aggregate shape on the properties of asphaltic concrete AC 14. *Jurnal Teknologi*, 71(3), 69–73. <https://doi.org/10.11113/jt.v71.3762>
- Jiang, J., Ni, F., Gao, L., & Yao, L. (2017). Effect of the contact structure characteristics on rutting performance in asphalt mixtures using 2D imaging analysis. *Construction and Building Materials*, 136, 426–435. <https://doi.org/10.1016/j.conbuildmat.2016.12.210>
- Lavin, P. G. (2003). *Asphalt pavements: A practical guide to design production, and maintenance for engineers and architects*. Spon Press, Taylor & Francis Group.
- Ling, C., & Bahia, H. (2020). Modelling of aggregates' contact mechanics to study roles of binders and aggregates in asphalt mixtures rutting. *Road Materials and Pavement Design*, 21(3), 720–736. <https://doi.org/10.1080/14680629.2018.1527716>

- Ljubic, A., & Prosen, J. (2004). *Resistance to permanent deformations in relation to asphalt mix composition*. Proceedings of the 3rd Euraspalt & Eurobitume Congress, Vienna.
- Miranda, H. M. B. (2016). *Stone mastic asphalt – mix design, production, application and performance* (Doctoral dissertation). Universidade de Lisboa, Instituto Superior Técnico, Lisbon (in Portuguese). <https://bibliotecas.utl.pt/cgi-bin/koha/opac-detail.pl?biblionumber=511696>
- Miranda, H. M. B., Batista, F., Antunes, M. L., & Neves, J. (2019). A new SMA mix design approach for optimisation of stone-on-stone effect. *Road Materials and Pavement Design*, 20(1), S462–S479. <https://doi.org/10.1080/14680629.2019.1588779>
- Miranda, H. M. B., Batista, F., Antunes, M. L., & Neves, J. (2020). Influence of laboratory aggregate compaction method on the particle packing of Stone Mastic Asphalt. *Manuscript submitted for publication*.
- Mirzahosseini, M., Najjar, Y. M., Alavi, A. H., & Gandomi, A. H. (2013). ANN-based prediction model for rutting propensity of asphalt mixtures. Proceedings of the 92nd Annual Meeting Transportation Research Board, Washington, DC.
- Moghaddam, T. B., & Baaj, H. (2018). Application of compressible packing model for optimization of asphalt concrete mix design. *Construction and Building Materials*, 159, 530–539. <https://doi.org/10.1016/j.conbuildmat.2017.11.004>
- Muraya, P. M. (2007). *Permanent deformation of asphalt mixtures* (Doctoral dissertation). Delf University. <http://resolver.tudelft.nl/uuid:2fb9695a-d0e8-46bf-94d1-6cdebd411712>
- Nahi, M. H., Kamaruddin, I., Ismail, A., & Al-Mansob, R. A. (2014). Finite element model for rutting prediction in asphalt mixes in various air void content. *Journal of Applied Sciences*, 14(21), 2730–2737. <https://doi.org/10.3923/jas.2014.2730.2737>
- Pan, T., Tutumluer, E., & Carpenter, S. H. (2006). Effect of coarse aggregate morphology on permanent deformation behavior of hot mix asphalt. *Journal of Transportation Engineering*, 132(7), 580–589. [https://doi.org/10.1061/\(ASCE\)0733-947X\(2006\)132:7\(580\)](https://doi.org/10.1061/(ASCE)0733-947X(2006)132:7(580))
- Pasetto, M., & Baldo, N. (2014). Influence of the aggregate skeleton design method on the permanent deformation resistance of stone mastic asphalt. *Materials Research Innovations*, 18(3), 96–101. <https://doi.org/10.1179/1432891714Z.000000000588>
- Roquier, G. (2019). A theoretical packing density model (TPDM) for ordered and disordered packings. *Powder Technology*, 344, 343–362. <https://doi.org/10.1016/j.powtec.2018.12.033>
- Shell. (2015). *The Shell bitumen handbook*. Thomas Telford.
- Vavrik, W. R., Huber, G. A., Pine, W. J., Carpenter, S. H., & Bailey, R. (2002). *Bailey method for gradation selection in hot-mix asphalt mixture design*. (Report No. E-C044). Transportation Research Board.
- Vavrik, W. R., Pine, W. J., Huber, G. A., Carpenter, S. H., & Bailey, R. (2001). The Bailey method of gradation evaluation: The influence of aggregate gradation and packing characteristics on voids in the mineral aggregate. *Journal of the Association of Asphalt Paving Technologists*, 70, 132–175.
- Voskuilen, J. (2000, May 9–10). *Ideas for a volumetric mix design method for stone mastic asphalt*. Proceedings of the 6th International Conference Durable and Safe Pavements, Kielce.
- Zhang, Y., Luo, X., Onifade, I., Huang, X., Lytton, R. L., & Birgisson, B. (2019). Mechanical evaluation of aggregate gradation to characterize load carrying capacity and rutting resistance of asphalt mixtures. *Construction and Building Materials*, 205, 499–510. <https://doi.org/10.1016/j.conbuildmat.2019.01.218>
- Zhao, Y. L. (2005). *Composition mechanism of asphalt mixtures* (Doctoral dissertation). Southeast University. https://www.seu.edu.cn/_web/search/doSearch.do?locale=en&_p=YXM9NCZ0PTE4NzUmZD02MTMyJnA9MSZtPVNOJg__